

# EViT: An Eagle Vision Transformer with Bi-Fovea Self-Attention

Yulong Shi<sup>1</sup>, Mingwei Sun<sup>1\*</sup>, Yongshuai Wang<sup>1</sup>, Rui Wang<sup>2</sup>, Hui Sun<sup>2</sup>, Zengqiang Chen<sup>1,3</sup>

<sup>1</sup>College of Artificial Intelligence, Nankai University, Tianjin 300350, China,

<sup>2</sup>College of Information Engineering and Automation, Civil Aviation University of China, Tianjin 300300, China,

<sup>3</sup>Key Laboratory of Intelligent Robotics of Tianjin, Tianjin 300350, China.

ylshi@mail.nankai.edu.cn, smw\_sunmingwei@163.com, wangys@nankai.edu.cn,

ruiwang@cauc.edu.cn, h-sun@cauc.edu.cn, nkugnw@gmail.com

## Abstract

*Thanks to the advancement of deep learning technology, vision transformer has demonstrated competitive performance in various computer vision tasks. Unfortunately, vision transformer still faces some challenges such as high computational complexity and absence of desirable inductive bias. To alleviate these problems, a novel Bi-Fovea Self-Attention (BFSA) is proposed, inspired by the physiological structure and characteristics of bi-fovea vision in eagle eyes. This BFSA can simulate the shallow fovea and deep fovea functions of eagle vision, enable the network to extract feature representations of targets from coarse to fine, facilitate the interaction of multi-scale feature representations. Additionally, a Bionic Eagle Vision (BEV) block based on BFSA is designed in this study. It combines the advantages of CNNs and Vision Transformers to enhance the ability of global and local feature representations of networks. Furthermore, a unified and efficient general pyramid backbone network family is developed by stacking the BEV blocks in this study, called Eagle Vision Transformers (EViT). Experimental results on various computer vision tasks including image classification, object detection, instance segmentation and other transfer learning tasks show that the proposed EViT performs effectively by comparing with the baselines under same model size and exhibit higher speed on graphics processing unit than other models. Code is available at <https://github.com/nkusyl/EViT>.*

**Keywords:** Bi-Fovea Self-Attention, Bionic Eagle Vision, Eagle Vision Transformer.

## 1. Introduction

Since 2012, Convolutional Neural Networks (CNNs) have been dominating in various computer vision tasks due

to their inherent inductive biases, such as translation invariance and local sensitivity. However, it is difficult for CNNs to perceive the global feature dependencies of images, because of the limited receptive field of convolution kernels. This issue restricts the further development and applications of CNNs [26, 55]. Meanwhile, the rapid development of Transformer [47] in Natural Language Processing (NLP) has attracted worldwide attention from computer vision researchers [15, 22]. Compared with the CNNs, Transformers are excellent at modeling global feature dependencies and capturing contextual information [12, 63]. These two factors are critical for improving the performance of networks in image classification [1, 5], object detection [4, 68], and other vision tasks [17, 20, 57].

Inspired by the success of Transformer [47] in NLP, researchers have also attempted to apply Transformer to computer vision tasks. Unlike NLP, Vision Transformer (ViT) [9] splits input images into sequences and converts them into sequential data. Multi-Head Self-Attention (MHSA) is then utilized to capture global feature dependencies in images, generate effective feature representations for image classification task and achieve comparable performance to state-of-the-art CNNs. Subsequently, various vision transformer variants [10, 31, 45, 58] have been proposed, to provide new paradigms and solutions to computer vision tasks, breaking the monopoly of CNNs in computer vision tasks [31, 36, 41]. Nonetheless, the vision transformer models also meet several challenges, including: (1) Compared with CNNs, the MHSA in transformers has quadratic computational complexity and memory cost, the problem is especially prominent when dealing with high-resolution images and videos. (2) 2D input images should be converted into 1D input sequences. This process easily leads to networks insufficient ability for modeling spatially localized information and loss of relative positional relationships between features. (3) Due to the flexibility of MHSA and complexity of large-scale parameters, vision transformers lack appropriate inductive bias, to make the network tend to

\*Corresponding author.

overfit the training data.

To alleviate these problems, this paper draws inspiration from biological eagle vision system, hoping to design a bionic hybrid backbone network based on convolution and vision transformer. Although the eagle vision and vision transformer come from biological and computer sciences respectively, this paper still finds three similar features through analogy as follows. **(1) High resolution and sensitivity:** Eagle vision is known for its high resolution, wide field of view and keen sensitivity. This allows eagles to quickly capture small prey in vast field. Similarly, the vision transformer allows networks to focus on details in images, thereby capturing critical representations of targets for image classification and other vision tasks. **(2) Multi-level feature extraction:** Eagles process visual information at multiple levels, starting with photoreceptor cells and eventually reaching cerebral cortex. In similar, vision transformer extracts the target features layer by layer through stacking self-attention and Multi-Layer Perceptron (MLP). **(3) Global and local information awareness:** The bi-fovea structure of eagle vision can help eagles perceive global and local information about their surrounding environments, which helps them to track prey. The vision transformer also enable networks to establish associations among different regions of images, and to obtain the global and local feature representations of targets.

According to the discussion above, we design a Bionic Eagle Vision (BEV) block based on unique bi-fovea physiological structure and characteristics of eagle vision. This BEV block consists of Convolutional Positional Embedding (CPE), Bi-Fovea Self-Attention (BFSA) and Convolutional Feed-Forward Network (CFFN). Based on hierarchical design concepts [19, 49], a general vision backbone network framework is established, called Eagle Vision Transformer (EViT), by stacking multiple BEV blocks. Furthermore, the depth and width of the EViT is scaled, expanding it into a backbone network family comprising four variants: EViT-Tiny, EViT-Small, EViT-Base and EViT-Large, to enhance applicability across various computer vision tasks. To the best of our knowledge, this is the first work to combine eagle vision with vision transformer on large-scale datasets such as ImageNet [37] and is also the first study to propose a general family of vision backbone networks based on eagle vision.

The main contributions are as follows.

- Benefiting from biological eagle vision, a novel Bi-Fovea Self-Attention (BFSA) is proposed to simulate the shallow-fovea and deep-fovea functions of eagle vision, especially to enhance the ability of networks to capture fine-grained feature representations of targets.
- As the foundation of BFSA, the BEV block is provided. This BEV block combines the advantages of CNNs and Vision Transformers to incorporate proper

inductive bias in networks, reducing networks depth and memory cost.

- A unified efficient general pyramid backbone network family, EViTs, is proposed. It has good generalization capability and superiority in image classification, object detection, instance segmentation and other transfer learning tasks, especially in achieving a better trade-off between computational accuracy and efficiency.

The remainder of this paper is structured as follows. Section 2 summarizes the related work of this paper in biological eagle vision and vision transformer, respectively. Section 3 describes the design process of EViTs. Section 4 shows the experimental results of EViTs on various vision tasks. Section 5 is the conclusion.

## 2. Related Work

### 2.1. Eagle Vision Mechanism

It is widely known that eagle possesses an excellent natural visual system, with keen observation of the environment [32]. Figure 1 shows the physiological structure and photoreceptor cell density distribution of the bi-fovea in eagle eyes. According to Figure 1, the eagle eyes have two distinct foveas, namely the deep fovea and the shallow fovea. The deep fovea is located at the center of the retina and has high density of photoreceptor cells, which are crucial to improve the visual resolution of eagle eyes, allowing eagles to recognize prey at long distances and capture them [11]. The shallow fovea is in the peripheral area of the retina and has relatively low density of photoreceptor cells, however can provide a wider field of view [2].

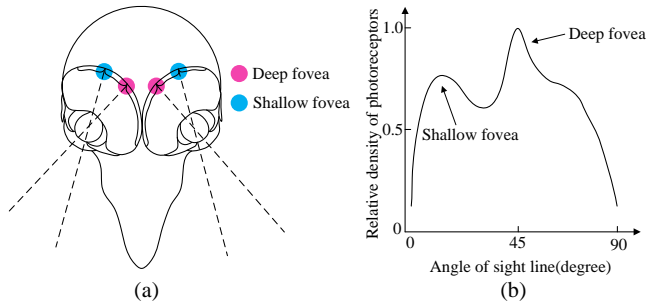


Figure 1. (a) the physiological structure of the bi-fovea in eagle eyes; (b) the density distribution of photoreceptor cells in bi-fovea.

Although one eye of eagles cannot use deep fovea and shallow fovea for imaging at the same time, it is worth noting that the eagle two eyes can collaborate, alternating between the deep fovea and shallow fovea to image [2]. For example, when an eagle looks ahead, the deep fovea of one eye is used for fine target recognition, at same time the shallow fovea of the other eye can be used to perceive the surrounding environment. This paper refers the above-

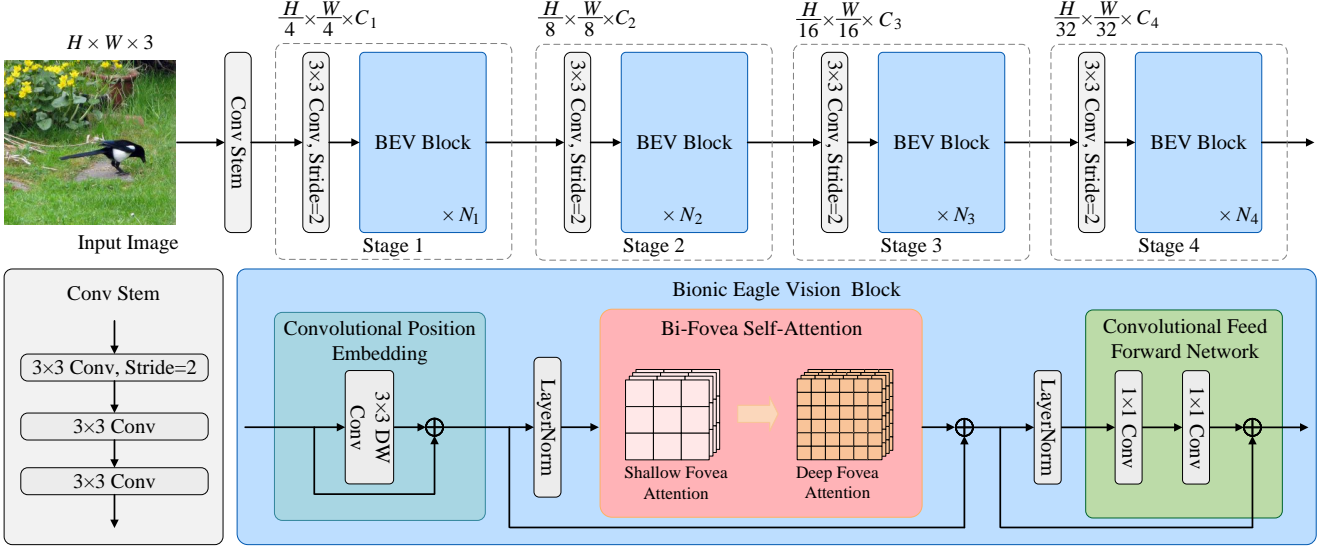


Figure 2. Illustration of the EViT. EViT is composed of a convolutional stem, multiple  $3 \times 3$  convolution layers with stride 2 and BEV blocks. A BEV block consists of CPE, BFSA and CFFN.

mentioned eagle vision characteristic as interaction mechanism. Based on this observation, we propose a novel BFSA module for simulating the shallow fovea and deep fovea of eagle vision, enabling network to capture the feature representation of targets from coarse to fine, which is valuable for vision tasks.

## 2.2. Transformers for Vision

Transformer is a self-attention model that was originally designed and applied for machine translation tasks, and it has shown impressive performance [47]. Subsequently, various transformer variants have been proposed and have made great progress in the field of natural language processing [3, 8, 51]. ViT [9] is a pioneering work that introduces transformer into vision tasks, which only consists of transformer encoder and patch embedding. Compared with CNNs, the essential difference is that vision transformer employs MHSA as an alternative to convolution for global context modeling. Following ViT, a series of improvement methods have been proposed [16, 31, 59], driving the rapid development of Transformer in computer vision. During the training phase, DeiT [42] employs the idea of knowledge distillation by introducing distillation tokens into the input sequence of encoder to guide the learning process of transformer. CvT [52] utilizes convolutional token embedding and convolutional projection in the transformer framework to obtain local context information and global relative positional relationships of feature sequences. Subsequent works [7, 48, 65] incorporates convolution into the early stages of the transformer to improve the stability of model training. CMT [13] and PVT [49] are hybrid models of CNNs and Transformers to mitigate the memory cost of multi-head self-attention, which use depth-wise convolution

to reduce the spatial size of the feature token before the projection operation. In this work, we demonstrate the potential of combining eagle vision with vision transformer, and we expect that EViT can bring more performance breakthroughs in vision tasks.

## 3. Approach

### 3.1. Overall Architecture

Taking inspiration from recent transformer models, we introduce a novel CNNs and Transformers hybrid network family based on eagle vision properties, called Eagle Vision Transformers (EViT). We wish to take advantages of CNNs and Transformers to alleviate the high computational complexity of MHSA, and to introduce desirable inductive biases in EViT. The overall pipeline of EViT is illustrated in Figure 2. Given an input image of size  $H \times W \times 3$ , it is first fed into the convolutional stem to obtain the low-level feature representations. This convolutional stem follows the previous works [21, 25], employing three successive  $3 \times 3$  convolution layers at early stage to stabilize the training process of the network, wherein the first convolution layer is with stride 2. Then, these low-level representations are processed through a series of  $3 \times 3$  convolution layers and BEV blocks to generate hierarchical representations of targets, which is crucial for vision dense prediction tasks. It is worth noting that these  $3 \times 3$  convolutional layers are used for patch embedding to adjust the feature dimensions and reduce the resolution of input tokens. As a backbone network for multiple vision tasks, we follow the standard pyramid four-stage design [19, 49]. Each stage has similar architecture, which contains a  $3 \times 3$  convolution layer with stride 2 and  $N_i$  BEV blocks. The difference are that the res-

olutions of the output features for stage 1 stage 4 are divided by factors of 4, 8, 16 and 32, respectively, and the corresponding channel dimensions are increased to  $C_1$ ,  $C_2$ ,  $C_3$  and  $C_4$ , respectively. Finally, in image classification task, we use  $1 \times 1$  convolution projection, average pooling layer and fully connected layer as classifier to output the predictions.

### 3.2. Bionic Eagle Vision Block

As the basic building block of EViT, the BEV block combines the advantages of CNNs and Transformers. A BEV block consists of three key components: Convolutional Positional Embedding (CPE), Bi-Fovea Self-Attention (BFSA) and Convolutional Feed-Forward Network (CFFN). The complete mathematical definition of BEV block is shown as

$$\mathbf{X} = \text{CPE}(\mathbf{X}_{in}) + \mathbf{X}_{in} \quad (1)$$

$$\mathbf{Y} = \text{BFSA}(\text{LN}(\mathbf{X})) + \mathbf{X} \quad (2)$$

$$\mathbf{Z} = \text{CFFN}(\text{LN}(\mathbf{Y})) + \mathbf{Y} \quad (3)$$

where, LN is LayerNorm function, which is used to normalize the feature tensors. Taking stage 1 as an example. When a token tensor  $\mathbf{X}_{in} \in \mathbb{R}^{H \times W \times C}$  is input into the BEV block, which first uses CPE to introduce feature location information into all tokens. Compared with Absolute Position Embedding (APE) [31] and Relative Position Embedding (RPE) [38], CPE can flexibly learn the position information of arbitrary resolution features by zero padding of convolutional function. Then, this block employs BFSA module to simulate the shallow fovea and deep fovea of eagle vision for modeling the global feature dependencies and local fine-grained feature representations in images, and achieving the interactive fusion of these two representations. The details of BFSA will be elaborated in the following subsection. Finally, we use two  $1 \times 1$  convolutional layers as CFFN to further enhance the feature representation of each token.

### 3.3. Bi-Fovea Self-Attention

Figure 1 shows the physiological structure and photoreceptor cell density distribution of bi-fovea in eagle eyes. Relatively speaking, the shallow fovea of eagle vision is used for coarse-grained environmental perception, and the deep fovea is used for fine-grained prey recognition. Taking inspiration from this fact, we expect to establish a similar module as bi-fovea in eagle eyes. This leads to the Bi-Fovea Self-Attention (BFSA). The BFSA consists of two Token Interaction Fusion (TIF) modules, a Local Information Awareness (LIA) module, a Shallow Fovea Attention (SFA) and a Deep Fovea Attention (DFA). Similar to the bi-fovea vision of eagle eyes, we use the SFA to model the

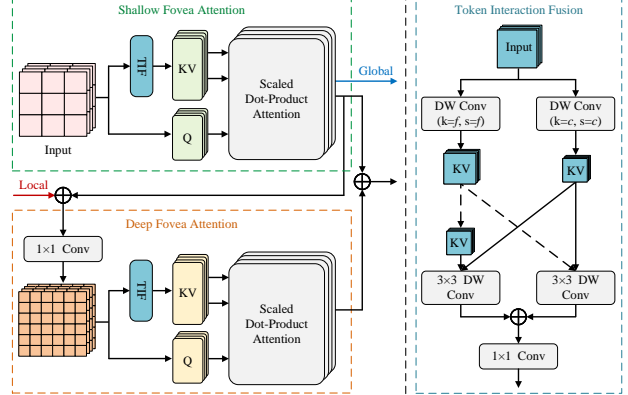


Figure 3. Illustration of the BFSA. The BFSA consists of two Token Interaction Fusion (TIF) module, a Shallow Fovea Attention (SFA) and a Deep Fovea Attention (DFA)

global feature dependencies of images, and the DFA to capture fine-grained feature representations of targets. The illustration of this BFSA module is shown in Figure 3

**Shallow Fovea Attention.** In original Multi-Head Self-Attention (MHSA), the token tensor  $\mathbf{X}' \in \mathbb{R}^{H \times W \times C}$  is first projected into Query  $\mathbf{Q} \in \mathbb{R}^{N \times D}$ , Key  $\mathbf{K} \in \mathbb{R}^{N \times D}$  and Value  $\mathbf{V} \in \mathbb{R}^{N \times D}$ , where  $N$  and  $D$  are the length and dimension of the input token sequence, respectively. To alleviate the computational complexity and memory cost of MHSA, a Token Interaction Fusion (TIF) module is first designed based on depth-wise convolution and  $1 \times 1$  convolution, which is used to reduce the spatial sizes of  $\mathbf{K}$  and  $\mathbf{V}$  prior to the projection operation. The structure of this TIF is shown in Figure 3, where the dotted arrows denote the down-sampling of the feature representations by using  $3 \times 3$  depth-wise convolution with stride 2 and padding 1. It has two parameters,  $c$  and  $f$ , which are used to control the reduced size of feature tokens. In addition, TIF can also achieve the extraction and interaction of multi-scale feature tokens, which is particularly crucial for vision dense prediction tasks.

Furthermore, we take  $\mathbf{Q}' = \text{Linear}(\mathbf{X}')$ ,  $\mathbf{K}' = \text{Linear}(\text{TIF}(\mathbf{X}'))$  and  $\mathbf{V}' = \text{Linear}(\text{TIF}(\mathbf{X}'))$  as inputs and then use multi-head self-attention to model the global feature dependencies among all the tokens to yield attention scores. The compact matrix form of the SFA is defined as

$$\text{SFA}(\mathbf{X}') = \text{Concat}(\mathbf{head}_0, \mathbf{head}_1, \dots, \mathbf{head}_h) \mathbf{W}^o \quad (4)$$

$$\mathbf{head}_i = \text{Attention}(\mathbf{Q}_i, \mathbf{K}'_i, \mathbf{V}'_i) \quad (5)$$

$$\text{Attention}(\mathbf{Q}, \mathbf{K}', \mathbf{V}') = \text{softmax}\left(\frac{\mathbf{Q}\mathbf{K}'^T}{\sqrt{D}}\right)\mathbf{V}' \quad (6)$$

where  $\mathbf{head}_i \in \mathbb{R}^{N \times \frac{D}{h}}$  is the output of the  $i^{th}$  attention head, and the weight matrix  $\mathbf{W}^o \in \mathbb{R}^{N \times \frac{D}{h}}$  is used to compose all heads.

Table 1. Four architectural variants of EViT for ImageNet classification.  $H_i$  denotes the number of attention heads in DFA and SFA of stage  $i$ .  $c_i$  and  $f_i$  are used to control the reduced size of feature tokens of stage  $i$ .  $r_i$  denotes the expansion ratio in CFFN of stage  $i$ .

Output size	Layer Name	EViT-Tiny	EViT-Small	EViT-Base	EViT-Large
112 × 112	Conv Stem	$3 \times 3, 24, \text{stride } 2$ $[3 \times 3, 20] \times 2$	$3 \times 3, 28, \text{stride } 2$ $[3 \times 3, 24] \times 2$	$3 \times 3, 32, \text{stride } 2$ $[3 \times 3, 28] \times 2$	$3 \times 3, 32, \text{stride } 2$ $[3 \times 3, 32] \times 2$
56 × 56	Patch Embedding	$2 \times 2, 48, \text{stride } 2$	$2 \times 2, 56, \text{stride } 2$	$2 \times 2, 64, \text{stride } 2$	$2 \times 2, 64, \text{stride } 2$
Stage 1	BEV block	$\begin{bmatrix} H_1=1, c_1=8 \\ f_1=4, r_1=3 \end{bmatrix} \times 2$	$\begin{bmatrix} H_1=1, c_1=8 \\ f_1=4, r_1=3.5 \end{bmatrix} \times 2$	$\begin{bmatrix} H_1=1, c_1=8 \\ f_1=4, r_1=3.5 \end{bmatrix} \times 3$	$\begin{bmatrix} H_1=1, c_1=8 \\ f_1=4, r_1=4 \end{bmatrix} \times 4$
28 × 28	Patch Embedding	$2 \times 2, 96, \text{stride } 2$	$2 \times 2, 112, \text{stride } 2$	$2 \times 2, 128, \text{stride } 2$	$2 \times 2, 128, \text{stride } 2$
Stage 2	BEV block	$\begin{bmatrix} H_2=2, c_2=4 \\ f_2=2, r_2=3 \end{bmatrix} \times 2$	$\begin{bmatrix} H_2=2, c_2=4 \\ f_2=2, r_2=3.5 \end{bmatrix} \times 2$	$\begin{bmatrix} H_2=2, c_2=4 \\ f_2=2, r_2=3.5 \end{bmatrix} \times 3$	$\begin{bmatrix} H_2=2, c_2=4 \\ f_2=2, r_2=4 \end{bmatrix} \times 4$
14 × 14	Patch Embedding	$2 \times 2, 192, \text{stride } 2$	$2 \times 2, 224, \text{stride } 2$	$2 \times 2, 256, \text{stride } 2$	$2 \times 2, 256, \text{stride } 2$
Stage 3	BEV block	$\begin{bmatrix} H_3=4, c_3=2 \\ f_3=1, r_3=3 \end{bmatrix} \times 2$	$\begin{bmatrix} H_3=4, c_3=2 \\ f_3=1, r_3=3.5 \end{bmatrix} \times 6$	$\begin{bmatrix} H_3=4, c_3=2 \\ f_3=1, r_3=3.5 \end{bmatrix} \times 8$	$\begin{bmatrix} H_3=4, c_3=2 \\ f_3=1, r_3=4 \end{bmatrix} \times 10$
7 × 7	Patch Embedding	$2 \times 2, 384, \text{stride } 2$	$2 \times 2, 448, \text{stride } 2$	$2 \times 2, 512, \text{stride } 2$	$2 \times 2, 512, \text{stride } 2$
Stage 4	BEV block	$\begin{bmatrix} H_4=8, c_4=1 \\ f_4=1, r_4=3 \end{bmatrix} \times 2$	$\begin{bmatrix} H_4=8, c_4=1 \\ f_4=1, r_4=3.5 \end{bmatrix} \times 2$	$\begin{bmatrix} H_4=8, c_4=1 \\ f_4=1, r_4=3.5 \end{bmatrix} \times 3$	$\begin{bmatrix} H_4=8, c_4=1 \\ f_4=1, r_4=4 \end{bmatrix} \times 4$
1 × 1	Projection			$1 \times 1, 1280$	
1 × 1	Classifier			Fully Connected Layer, 1000	
Params		12.67 M	24.10 M	42.47 M	55.71 M
FLOPs		1.71 G	3.53 G	6.23 G	8.16 G

**Deep Fovea Attention.** In DFA, the mathematical definitions of DFA and SFA are almost the same, and the only difference is the inputs. In order to incorporate proper inductive bias in BFSA and enhance its local feature representation ability, we design a Local Information Awareness (LIA) module via residual bottleneck connection [19]. The LIA consists of two  $1 \times 1$  convolutions and a  $3 \times 3$  depth-wise convolution. It encourages DFA to learn the intrinsic structural information and local relationships of each feature tokens. As a connection of local feature information between SFA and DFA, we take the output of SFA and the  $\mathbf{X}' \in \mathbb{R}^{H \times W \times C}$  as the input for LIA. The complete mathematical definition of LIA module is shown as

$$\text{LIA}(\mathbf{X}) = \text{Conv}(\text{DWConv}(\text{Conv}(\mathbf{X})) + \text{Conv}(\mathbf{X})) \quad (7)$$

where  $\mathbf{X} = \text{Concat}(\mathbf{X}' + \text{SFA}(\mathbf{X}'))$ , and the activation and normalization functions are omitted. We use the outputs of SFA and LIA as input to DFA, which is defined as

$$\mathbf{X}'' = \text{Conv}(\text{SFA}(\mathbf{X}') + \text{LIA}(\mathbf{X}' + \text{SFA}(\mathbf{X}'))) \quad (8)$$

Finally, we combine the outputs of SFA and DFA and feeds them to the next layer as

$$\mathbf{Out} = \text{Concat}(\text{SFA}(\mathbf{X}'_{in}) + \text{DFA}(\mathbf{X}''_{in})) \quad (9)$$

Algorithm 1 summarizes the calculation process of BFSA.

#### Algorithm 1 Bi-Fovea Self-Attention algorithm.

Input:  $\mathbf{X} \in \mathbb{R}^{H \times W \times C}$ ; Output:  $\mathbf{Y} \in \mathbb{R}^{H \times W \times C}$ .

# model feature global dependencies (GFD) using SFA

$\text{SFA}(\mathbf{X}) = \text{Concat}(\mathbf{head}_0, \mathbf{head}_1, \dots, \mathbf{head}_h) \mathbf{W}'$

$\mathbf{Q} = \text{Linear}(\mathbf{X})$ ,  $\mathbf{K}$ ,  $\mathbf{V} = \text{Linear}(\text{TIF}(\mathbf{X}))$

$\mathbf{head}_i = \text{Attention}(\mathbf{Q}_i, \mathbf{K}_i, \mathbf{V}_i)$

$\text{Attention}(\mathbf{Q}, \mathbf{K}, \mathbf{V}) = \text{softmax}\left(\frac{\mathbf{Q}\mathbf{K}^T}{\sqrt{D}}\right)\mathbf{V}$

# learn the intrinsic structural information and local

# relationships of all the features using LIA

$\mathbf{X}' = \text{Concat}(\mathbf{X} + \text{SFA}(\mathbf{X}))$

$\text{LIA}(\mathbf{X}') = \text{Conv}(\text{DWConv}(\text{Conv}(\mathbf{X}')) + \text{Conv}(\mathbf{X}'))$

# extract fine-grained features of targets using DFA and

# output the results of BFSA

$\mathbf{X}'' = \text{Conv}(\text{SFA}(\mathbf{X}') + \text{LIA}(\mathbf{X}' + \text{SFA}(\mathbf{X}')))$

$\text{DFA}(\mathbf{X}'') = \text{Concat}(\mathbf{head}'_0, \mathbf{head}'_1, \dots, \mathbf{head}'_h) \mathbf{W}''$

$\mathbf{Y} = \text{Concat}(\text{SFA}(\mathbf{X}) + \text{DFA}(\mathbf{X}''))$

#### 3.4. Architecture Variants of EViT

We use the BEV block as basic building block, and proposes a novel general vision pyramid backbone network family, called EViT. To facilitate comparison with other backbone networks under similar model size and computational complexity, we provide four variants. They are EViT-Tiny, EViT-Small, EViT-Base and EViT-Large. The structural details of EViT are shown in Table 1. These variants follow the dominant four-stage pyramid structure design, with each stage having different number of BEV blocks and

hidden feature dimensions to adapt to the needs of various vision tasks. The 3x3 convolution with stride 2 is used for patch embedding to connect these different stages such that the spatial size of feature maps are halved, and the dimensions are doubled before entering the next stage. Therefore, each stage can output feature maps of four different sizes to obtain rich hierarchical feature representations of targets. For the ease of understanding the implementation details of the four variants, we unify their input image resolutions to  $224^2$  in Table 1. Specially, the input image resolutions of EViT-Tiny, EViT-Small, EViT-Base and EViT-Large are  $160^2$ ,  $192^2$ ,  $224^2$ , and  $256^2$  respectively, during the training process.

## 4. Experiments

To evaluate the effectiveness of EViT, we apply EViT to a series of mainstream computer vision tasks, including ImageNet-1K [37] classification (Sec. 4.1), COCO 2017 [29] object detection and instance segmentation (Sec. 4.2), and other transfer learning tasks (Sec. 4.3). Specifically, the EViT are trained first from scratch on ImageNet-1K dataset to implement image classification and obtain the pre-training parameters. Subsequently, the pre-training parameters of EViT are fine-tuned on object detection and other vision tasks respectively through transfer learning, which is used to validate the generalization performance of EViT. Additionally, the ablation experiments are conducted for EViT in Sec. 4.4. It is used to demonstrate the effectiveness of BFSA and TIF.

### 4.1. Image Classification on ImageNet-1k

**Settings.** In this section, the EViT are first evaluated on the ImageNet-1K [37] dataset, which contains 1000 classes with total of about 1.33M images, while the training dataset has about 1.28M images and the validation dataset has 50K images. For fairness, we follow the same training strategy as DeiT [42] and PVT [49] to compare with other methods. Specifically, we take AdamW as network parameter optimizer and the weight decay is set to 0.05. All models are trained 300 epochs and the initial learning rate is set to 0.001 with following cosine decay. We employ the same data augmentation techniques as DeiT [42], including random flipping, random cropping, random erasing [67], Cut-Mix [61], Mixup [62] and label smoothing [39]. The input image resolutions of these four network variants are  $160^2$ ,  $192^2$ ,  $224^2$ , and  $256^2$  respectively, during the training process.

**Results.** In this experiment, the EViT are compared with other popular CNN and vision transformer models, and the experimental results are shown in Table 2, which show that EViT obtain the best accuracy and speed trade-off compared with other methods under similar model parameters. Specifically, EViT-Tiny and EViT-Small exhibit better per-

Table 2. ImageNet-1K classification results of EViT. We group similar CNNs and Transformers together based on model parameters and classification performance. The proposed EViT consistently outperform other methods and with less computational cost.

Model	Resolution	FLOPs (G)	Params (M)	Top-1 Acc (%)
ResNet-18 [19]	$224^2$	1.8	11.7	69.8
RegNet-Y-1.6G [35]	$224^2$	1.6	11.2	78.0
PVT-T [49]	$224^2$	1.9	13.2	75.1
PVTv2-b1 [50]	$224^2$	2.1	13.1	78.7
PyramidTNT-Ti [14]	$224^2$	0.6	<b>10.6</b>	75.2
CoaT-Lite Mini [54]	$224^2$	2.0	11.0	78.9
EfficientViT-M5 [30]	$224^2$	<b>0.5</b>	12.4	77.1
LocalViT-PVT [27]	$224^2$	4.8	13.5	78.2
EViT-Tiny	$160^2$	0.8	12.6	<b>79.8</b>
ResNet-50 [19]	$224^2$	4.1	25.6	79.0
DeiT-S [42]	$224^2$	4.6	22.1	79.8
PVT-S [49]	$224^2$	3.7	24.5	79.8
T2T-14 [60]	$224^2$	5.2	<b>20.0</b>	81.5
TNT-S [16]	$224^2$	5.2	23.8	81.3
PVT-S [49]	$224^2$	3.8	24.5	79.8
LocalViT-S [27]	$224^2$	4.6	22.4	80.8
Swin-T [31]	$224^2$	4.5	28.3	81.3
CvT-13 [52]	$224^2$	4.5	<b>20.0</b>	81.6
EViT-Small	$192^2$	<b>2.6</b>	24.1	<b>82.1</b>
ResNet-101 [19]	$224^2$	7.9	45.0	77.4
RegNet-Y-8G [35]	$224^2$	8.0	39.2	79.9
PVT-M [49]	$224^2$	6.4	44.2	81.2
Swin-S [31]	$224^2$	8.7	49.6	83.3
NestT-Small [66]	$224^2$	10.4	38	83.3
CvT-21 [52]	$384^2$	24.9	<b>31.5</b>	83.3
MViT-B [10]	$224^2$	7.8	37	81.0
CViT-18 [5]	$224^2$	9.0	43	82.5
ViL-Medium [64]	$224^2$	9.1	39.7	83.3
EViT-Base	$224^2$	<b>6.2</b>	42.5	<b>84.1</b>
ResNet-152 [19]	$224^2$	11.6	60.0	82.0
T2T-24 [60]	$224^2$	14.1	64	82.3
TNT-B [16]	$224^2$	14.1	65.6	82.8
PVT-L [49]	$224^2$	9.8	61.4	81.7
PVT v2-B4 [50]	$224^2$	10.1	62.6	83.6
CaiT-S36 [43]	$224^2$	13.9	68	83.3
NestT-Base [66]	$224^2$	17.9	68	83.8
EViT-Large	$224^2$	<b>8.1</b>	<b>55.7</b>	<b>84.5</b>
EViT-Large	$256^2$	<b>10.8</b>	<b>55.7</b>	<b>85.1</b>

formance with smaller input image resolutions and fewer model parameters, achieving 79.8% and 82.1% classification accuracy respectively. Compared with Swin-S [31], NestT-Small [66], CvT-21 [52], and ViL-Medium [64], EViT-Base shows impressive performance with the lowest computational cost. Specifically, EViT-Base yields 84.1% Top-1 accuracy with 6.2 GFLOPs, which improves the performance by 0.8% over the four mentioned methods, and reduces nearly 1.5 to 5 times of computational complexity at the same time. At larger model scales, EViT-Large maintains significant competitive advantages over other existing methods. In particular, for fair comparison with other methods, we conduct two experiments on EViT-Large in image classification at  $224^2$  and  $256^2$  image sizes. At the same settings, EViT-Large can obtain 2.8% and 1.2% performance gains compared to PVT-L [49] and CaiT-S36 [43], respectively. When the input image size is set to  $256^2$ , the computational complexity and model parameters of EViT-Large are only 10.8 GFLOPs and 59.3M respectively, however it can obtain 85.1% classification performance. Based on the above experimental results, we observe that EViT exhibits

Table 3. Performance comparison of object detection (left group) and instance segmentation (right group) on the COCO 2017 val dataset. Each model is used as a visual backbone and then plugged into the RetinaNet [28] and Mask R-CNN [18] frameworks.

Backbone	Params (M)	RetinaNet					Params (M)	Mask R-CNN						
		<i>mAP</i>	$AP_{50}$	$AP_{75}$	$AP_S$	$AP_M$	$AP_L$	<i>mAP<sup>b</sup></i>	$AP_{50}^b$	$AP_{75}^b$	<i>mAP<sup>m</sup></i>	$AP_{50}^m$	$AP_{75}^m$	
ResNet-50 [19]	37.7	36.3	55.3	38.6	19.3	40.0	48.8	44.2	38.0	58.6	41.4	34.4	55.1	36.7
Swin-T [31]	38.5	41.5	62.1	44.2	25.1	44.9	55.5	47.8	42.2	64.6	46.2	39.1	61.6	42.0
DAT-T [53]	38.0	42.8	64.4	45.2	28.0	45.8	57.8	48.0	44.4	67.6	48.5	40.4	64.2	43.1
ResT-Base [65]	40.5	42.0	63.2	44.8	29.1	45.3	53.3	49.8	41.6	64.9	45.1	38.7	61.6	41.4
PVT-T [49]	34.2	40.4	61.3	43.0	25.0	42.9	55.7	44.1	40.4	62.9	43.8	37.8	60.1	40.3
PVTv2-B2 [50]	35.1	44.6	65.6	47.6	27.4	48.8	58.6	45.0	45.3	67.1	49.6	41.2	64.2	44.4
EViT-Small	<b>31.9</b>	<b>45.2</b>	<b>66.1</b>	<b>48.8</b>	<b>28.4</b>	<b>49.2</b>	<b>59.7</b>	<b>41.7</b>	<b>46.6</b>	<b>68.3</b>	<b>50.2</b>	<b>42.3</b>	<b>65.5</b>	<b>45.3</b>
ResNet-101 [19]	56.7	38.5	57.8	41.2	21.4	42.6	51.1	63.2	40.4	41.1	44.2	36.4	57.7	38.8
Swin-S [31]	59.8	44.5	65.7	47.5	27.4	48.0	59.9	69.1	44.8	66.6	48.9	40.9	63.4	44.2
DAT-S [53]	60.0	45.7	67.7	48.5	30.5	49.3	61.3	69.0	47.1	69.9	51.5	42.5	66.7	45.4
PVT-M [49]	53.9	41.9	63.1	44.3	25.0	44.9	57.6	63.9	42.0	64.4	45.6	39.0	61.6	42.1
PVTv2-B3 [50]	55.0	45.9	66.8	49.3	28.6	49.8	61.4	64.9	47.0	68.1	51.7	42.5	65.7	45.7
EViT-Base	<b>50.4</b>	<b>46.8</b>	<b>68.3</b>	<b>50.7</b>	<b>30.9</b>	<b>51.2</b>	<b>62.3</b>	<b>60.1</b>	<b>47.9</b>	<b>69.2</b>	<b>52.5</b>	<b>43.5</b>	<b>66.4</b>	<b>46.6</b>

significant advantages, particularly in terms of low computational complexity and scalability. In regard to computational complexity, we introduce convolutional operations into the EViTs, and design a TIF module to reduce the size of feature tokens in BFSA and decrease the computational complexity of EViTs. Concerning scalability, EViTs can be flexibly scaled to smaller or larger models depending on specific task requirements.

## 4.2. Object Detection and Instance Segmentation

**Settings.** In this section, we conduct object detection and instance segmentation experiments for EViTs on COCO 2017 [29] dataset. The COCO 2017 dataset contains 80 classes, 118k training images, 5k validation images and 20k test-dev images. We use two representative frameworks, RetinaNet [28] and Mask R-CNN [18] to evaluate the performance of EViTs. The EViTs are used as the vision backbone and then plugged into the RetinaNet and Mask R-CNN frameworks. Before training, we employ the pre-trained parameters on ImageNet-1k to initialize the EViTs backbone, and other layers are randomly initialized. For fairness, we follow the same settings as that of MMDection [6]: the short side of input images is resized to 800 and the long side is at most 1333; the AdamW is selected as optimizer and the training schedule is set to  $1 \times 12$  epochs; the weight decay and the initial learning rate are set to 0.05 and 0.0001, respectively.

**Results.** Table 3 shows the performance comparison of EViTs with other backbone networks for object detection and instance segmentation on COCO 2017 val dataset. For RetinaNet framework, the mean Average Precision (mAP), Average Precision at 50% and 75% IoU thresholds ( $AP_{50}$ ,  $AP_{75}$ ), and three object sizes Average Precision (small, medium, and large ( $AP_S$ ,  $AP_M$ , and  $AP_L$ )) are used as the evaluation metrics to evaluate model performance. From the results, it can be seen that EViTs have significant competitive advantages compared with other methods. Specifically, the average accuracy of EViT-Small and EViT-Base

Table 4. Details of used vision datasets. This table contains the number of classes, training images, and testing images for these datasets.

dataset	application	classes	train data	val data
Standford Cars [23]	fine-grained	196	8133	8041
Oxford-102 Flowers [33]	visual	102	2040	6149
Oxford-IIIT-Pets [34]	classification	37	3680	3669
iNaturalist18 [46]	long-tailed	8142	437513	24426
iNaturalist19 [46]	classification	1010	265240	3003
CIFAR10 [24]	superordinate	10	50000	10000
CIFAR100 [24]	classification	100	50000	10000

is at least 8% higher than those of the ResNet-50 and ResNet-101, and also surpasses the advanced PVTv2-B2 and PVTv2-B3 by 0.6% and 0.9%, respectively. For Mask R-CNN framework, the bounding box Average Precision ( $AP_b$ ) and mask Average Precision ( $AP_m$ ) at mean and different IoU thresholds (50%, 75%) are used as the evaluation metrics. According to the results, EViT-Small and EViT-Base also significantly outperform the other methods. Specifically, in  $mAP^b$  and  $mAP^m$  metrics, EViT-Small is ahead of PVTv2-B2 2.5%, 2.0% and EViT-Base is ahead of PVTv2-B3 1.6%, 1.2% respectively.

## 4.3. Other vision transfer learning tasks

**Settings.** In this section, other transfer learning experiments are conducted to evaluate the performance of EViTs in different downstream vision tasks. These vision tasks consist of different application scenarios and datasets, including fine-grained visual classification (Standford Cars [23], Oxford-102 Followers [33] and Oxford-IIIT-Pets [34]), long-tailed classification (iNaturalist18 [46], iNaturalist19 [46]) and superordinate classification (CIFAR10 [24], CIFAR100 [24]). The details of these datasets are listed in Table 4. For fairness, we follow the same settings as CMT [13]. Before training, we use the pre-trained parameters on ImageNet-1k to initialize the EViTs backbone, and other layers are randomly initialized.

**Results.** Table 5 shows the performance comparison be-

Table 5. Performance comparison between EViTs and other backbone networks on fine-grained visual classification task, long-tailed classification task and superordinate classification task.

Model	Params (M)	FLOPs (G)	Cars	Flowers	Pets	iNaturalist18	iNaturalist19	CIFAR10	CIFAR100
Grafit ResNet-50 [44]	25.6	4.1	92.5%	98.2%	-%	-%	75.9%	-%	-%
EfficientNet-B5 <sub>↑456</sub> [40]	28.0	10.3	93.9%	98.5%	94.9%	-%	-%	98.7%	91.1%
CeIT-S [59]	24.2	4.8	94.1%	98.6%	94.9%	73.3%	78.9%	<b>99.1%</b>	90.8%
TNT-S <sub>↑384</sub> [16]	23.8	5.2	-%	<b>98.8%</b>	94.7%	-%	-%	98.7%	90.1%
ViTAE-S [56]	23.6	5.6	91.4%	97.8%	94.2%	-%	76.0%	98.8%	90.8%
<b>EViT-Small</b>	24.1	<b>2.6</b>	<b>94.3%</b>	98.7%	<b>95.1%</b>	<b>73.4%</b>	<b>79.1%</b>	<b>99.1%</b>	<b>91.4%</b>
TNT-b <sub>↑384</sub> [16]	65.6	14.1	-%	99.0%	95.0%	-%	-%	99.1%	91.1%
EfficientNet-B7 <sub>↑600</sub> [40]	64.0	37.2	94.7%	<b>98.8%</b>	<b>95.4%</b>	-%	-%	98.9%	<b>91.7%</b>
ViT-B/16 <sub>↑384</sub> [9]	85.8	17.6	-%	89.5%	93.8%	-%	-%	98.1%	87.1%
DeiT-B [42]	85.8	17.3	92.1%	98.4%	-%	73.2%	77.7%	99.1%	90.8%
<b>EViT-Base</b>	42.5	<b>6.2</b>	<b>94.8%</b>	<b>98.8%</b>	95.3%	<b>73.7%</b>	<b>79.6%</b>	<b>99.3%</b>	<b>91.7%</b>

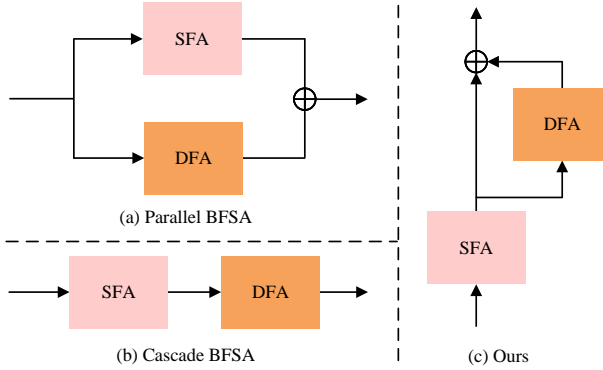


Figure 4. The three connection methods of BFSA.

tween EViTs and other backbone networks on these above vision tasks. As can be seen from the results, EViTs exhibit extremely competitive performance. In particular, EViTs achieves comparable performance to EfficientNet-B7 with the least computational cost and outperforms other CNNs and Transformers in classification accuracy. This demonstrates the superiority and generality of the EViTs based on eagle bi-foveal vision designed in this paper.

#### 4.4. Ablation Study

**Settings.** In this section, the ablation experiments are conducted for EViTs by using ImageNet-1K image classification dataset to demonstrate the effectiveness of BFSA and TIF. EViT-Base is considered for use in this ablation study. Specifically, the input image size is set to 224<sup>2</sup>, and the depth and width of the EViT-Base are kept constant as in Table 1.

**Structural analysis of the BFSA.** A major contribution of this paper is the design of Bi-Fovea Self-Attention (BFSA) through the incorporation of eagle vision interaction mechanisms. It achieves excellent performance in various vision tasks, such as image classification, object detection, and instance segmentation. This largely relies on the design ideas and structure of the BFSA. Figure 4 (c) shows the unique connection method of Shallow Fovea Attention

Table 6. Results of the ablation experiments for BFSA and TIF.

Method	FLOPs (G)	Params (M)	Top-1 Acc (%)
Parallel BFSA	5.7	40.0	81.6
Cascade BFSA	5.9	41.3	82.3
BFSA (Ours)	6.2	42.5	84.1
CSR	6.1	39.9	83.7
TIF	6.2	42.5	84.1

(SFA) and Deep Fovea Attention (DFA) in BFSA by simplification. According to Figure 4, the BFSA does not simply connect SFA and DFA in parallel or cascade, it is more like a combination of the two. Therefore, we first investigate the structure of the BFSA, which is used to demonstrate the effectiveness of this connection method. In the implementation details, we implement Parallel BFSA and Cascade BFSA by parallel connection and cascade connection between SFA and DFA, respectively. These are used to compare with the proposed BFSA scheme. Table 6 shows the performance comparison of the three connections for BFSA. As can be seen from the results, although ours BFSA is slightly higher than the Parallel BFSA and Cascade BFSA in computational complexity and parameters, it has significant advantages in performance. Specifically, in terms of the image classification accuracy, the BFSA outperforms parallel BFSA and cascaded BFSA by 2.5% and 1.2%, respectively. It can be shown that the superiority of the unique structural design in BFSA.

**Effectiveness analysis of TIF.** In subsection 3.3, a Token Interaction Fusion (TIF) module is designed for reducing the feature tokens sizes. This TIF not only can alleviate the computational complexity of BFSA, but also can facilitate the interaction and fusion of multi-scale feature tokens. To demonstrate the effectiveness of TIF, an ablation experiment for the TIF is conducted. Note that we follow PVT [49] by using a convolution layer to reduce the spatial size of feature tokens. For ease of analysis, we denote the method as Convolutional Spatial Reduction (CSR). Table 6 shows the performance comparison between TIF and CSR. It can be seen from the results, the TIF achieves 0.4% per-

formance improvement with only 2.6M parameter cost and negligible computational complexity, demonstrating the effectiveness of TIF.

## 5. Conclusion

A novel Bi-Fovea Self-Attention (BFSA) was proposed with its core idea derived from the interaction mechanism of bi-fovea vision in eagle eyes. It could help networks to extract fine-grained feature representations of targets while modelling the global feature dependencies of images. Furthermore, a Bionic Eagle Vision (BEV) block was designed based on BFSA in this study. This BEV block combines the advantages of CNNs and Transformers and was used as basic block to build the Eagle Vision Transformers (EViT). The EViT is a novel pyramid general vision backbone network framework, which contains four variants EViT-Tiny, EViT-Small, EViT-Base and EViT-Large. The experimental results showed that EViT can be effectively used as the backbone for various mainstream vision tasks, and has excellent performance in image classification, object detection and instance segmentation tasks. Especially in terms of computational complexity, EViT have significant competitive advantage compared with other CNN and Transformer models.

## Acknowledgement

This work was supported by the National Natural Science Foundation of China (Grant No. 62073177 and 61973175).

## References

- [1] Srinadh Bhojanapalli, Ayan Chakrabarti, Daniel Glasner, Daliang Li, Thomas Unterthiner, and Andreas Veit. Understanding robustness of transformers for image classification. In *Proceedings of the IEEE/CVF International Conference on Computer Vision*, pages 10231–10241, 2021. 1
- [2] Andreas Bringmann. Structure and function of the bird fovea. *Anatomia, Histologia, Embryologia*, 48(3):177–200, 2019. 2
- [3] Tom Brown, Benjamin Mann, Nick Ryder, Melanie Subbiah, Jared D Kaplan, Prafulla Dhariwal, Arvind Neelakantan, Pranav Shyam, Girish Sastry, Amanda Askell, et al. Language models are few-shot learners. *Advances in Neural Information Processing Systems*, 33:1877–1901, 2020. 3
- [4] Nicolas Carion, Francisco Massa, Gabriel Synnaeve, Nicolas Usunier, Alexander Kirillov, and Sergey Zagoruyko. End-to-end object detection with transformers. In *European Conference on Computer Vision*, pages 213–229. Springer, 2020. 1
- [5] Chun-Fu Richard Chen, Quanfu Fan, and Rameswar Panda. Crossvit: Cross-attention multi-scale vision transformer for image classification. In *Proceedings of the IEEE/CVF International Conference on Computer Vision*, pages 357–366, 2021. 1, 6
- [6] Kai Chen, Jiaqi Wang, Jiangmiao Pang, Yuhang Cao, Yu Xiong, Xiaoxiao Li, Shuyang Sun, Wansen Feng, Ziwei Liu, Jiarui Xu, et al. Mmdetection: Open mmlab detection toolbox and benchmark. *arXiv preprint arXiv:1906.07155*, 2019. 7
- [7] Qiang Chen, Qiman Wu, Jian Wang, Qinghao Hu, Tao Hu, Errui Ding, Jian Cheng, and Jingdong Wang. Mixformer: Mixing features across windows and dimensions. In *Proceedings of the IEEE/CVF Conference on Computer Vision and Pattern Recognition*, pages 5249–5259, 2022. 3
- [8] Jacob Devlin, Ming-Wei Chang, Kenton Lee, and Kristina Toutanova. Bert: Pre-training of deep bidirectional transformers for language understanding. *arXiv preprint arXiv:1810.04805*, 2018. 3
- [9] Alexey Dosovitskiy, Lucas Beyer, Alexander Kolesnikov, Dirk Weissenborn, Xiaohua Zhai, Thomas Unterthiner, Mostafa Dehghani, Matthias Minderer, Georg Heigold, Sylvain Gelly, et al. An image is worth 16x16 words: Transformers for image recognition at scale. *arXiv preprint arXiv:2010.11929*, 2020. 1, 3, 8
- [10] Haoqi Fan, Bo Xiong, Karttikeya Mangalam, Yanghao Li, Zhicheng Yan, Jitendra Malik, and Christoph Feichtenhofer. Multiscale vision transformers. In *Proceedings of the IEEE/CVF International Conference on Computer Vision*, pages 6824–6835, 2021. 1, 6
- [11] Julio González-Martín-Moro, JL Hernández-Verdejo, and A Clement-Corra. The visual system of diurnal raptors: updated review. *Archivos de la Sociedad Espanola de Oftalmología (English Edition)*, 92(5):225–232, 2017. 2
- [12] Jiaqi Gu, Hyoukjun Kwon, Dilin Wang, Wei Ye, Meng Li, Yu-Hsin Chen, Liangzhen Lai, Vikas Chandra, and David Z Pan. Multi-scale high-resolution vision transformer for semantic segmentation. In *Proceedings of the IEEE/CVF Conference on Computer Vision and Pattern Recognition*, pages 12094–12103, 2022. 1
- [13] Jianyuan Guo, Kai Han, Han Wu, Yehui Tang, Xinghao Chen, Yunhe Wang, and Chang Xu. Cmt: Convolutional neural networks meet vision transformers. In *Proceedings of the IEEE/CVF Conference on Computer Vision and Pattern Recognition*, pages 12175–12185, 2022. 3, 7
- [14] Kai Han, Jianyuan Guo, Yehui Tang, and Yunhe Wang. Pyramidtn: Improved transformer-in-transformer baselines with pyramid architecture. *arXiv preprint arXiv:2201.00978*, 2022. 6
- [15] Kai Han, Yunhe Wang, Hanting Chen, Xinghao Chen, Jianyuan Guo, Zhenhua Liu, Yehui Tang, An Xiao, Chunjing Xu, Yixing Xu, et al. A survey on vision transformer. *IEEE Transactions on Pattern Analysis and Machine Intelligence*, 45(1):87–110, 2022. 1
- [16] Kai Han, An Xiao, Enhua Wu, Jianyuan Guo, Chunjing Xu, and Yunhe Wang. Transformer in transformer. *Advances in Neural Information Processing Systems*, 34:15908–15919, 2021. 3, 6, 8
- [17] Jianfeng He, Jiacheng Deng, Tianzhu Zhang, Zhe Zhang, and Yongdong Zhang. Hierarchical shape-consistent transformer for unsupervised point cloud shape correspondence. *IEEE Transactions on Image Processing*, 2023. 1

[18] Kaiming He, Georgia Gkioxari, Piotr Dollár, and Ross Girshick. Mask r-cnn. In *Proceedings of the IEEE International Conference on Computer Vision*, pages 2961–2969, 2017. 7

[19] Kaiming He, Xiangyu Zhang, Shaoqing Ren, and Jian Sun. Deep residual learning for image recognition. In *Proceedings of the IEEE Conference on Computer Vision and Pattern Recognition*, pages 770–778, 2016. 2, 3, 5, 6, 7

[20] Tzu-Chun Hsu, Yi-Sheng Liao, and Chun-Rong Huang. Video summarization with spatiotemporal vision transformer. *IEEE Transactions on Image Processing*, 2023. 1

[21] Huabo Huang, Xiaoqiang Zhou, Jie Cao, Ran He, and Tieniu Tan. Vision transformer with super token sampling. In *Proceedings of the IEEE/CVF Conference on Computer Vision and Pattern Recognition*, pages 22690–22699, 2023. 3

[22] Salman Khan, Muzammal Naseer, Munawar Hayat, Syed Waqas Zamir, Fahad Shahbaz Khan, and Mubarak Shah. Transformers in vision: A survey. *ACM Computing Surveys (CSUR)*, 54(10s):1–41, 2022. 1

[23] Jonathan Krause, Michael Stark, Jia Deng, and Li Fei-Fei. 3d object representations for fine-grained categorization. In *Proceedings of the IEEE International Conference on Computer Vision Workshops*, pages 554–561, 2013. 7

[24] Alex Krizhevsky, Geoffrey Hinton, et al. Learning multiple layers of features from tiny images. 2009. 7

[25] Youngwan Lee, Jonghee Kim, Jeffrey Willette, and Sung Ju Hwang. Mpvit: Multi-path vision transformer for dense prediction. In *Proceedings of the IEEE/CVF Conference on Computer Vision and Pattern Recognition*, pages 7287–7296, 2022. 3

[26] Wenshuo Li, Hanting Chen, Jianyuan Guo, Ziyang Zhang, and Yunhe Wang. Brain-inspired multilayer perceptron with spiking neurons. In *Proceedings of the IEEE/CVF Conference on Computer Vision and Pattern Recognition*, pages 783–793, 2022. 1

[27] Yawei Li, Kai Zhang, Jiezhang Cao, Radu Timofte, and Luc Van Gool. Localvit: Bringing locality to vision transformers. *arXiv preprint arXiv:2104.05707*, 2021. 6

[28] Tsung-Yi Lin, Priya Goyal, Ross Girshick, Kaiming He, and Piotr Dollár. Focal loss for dense object detection. In *Proceedings of the IEEE International Conference on Computer Vision*, pages 2980–2988, 2017. 7

[29] Tsung-Yi Lin, Michael Maire, Serge Belongie, James Hays, Pietro Perona, Deva Ramanan, Piotr Dollár, and C Lawrence Zitnick. Microsoft coco: Common objects in context. In *Computer Vision–ECCV 2014: 13th European Conference, Zurich, Switzerland, September 6–12, 2014, Proceedings, Part V I3*, pages 740–755. Springer, 2014. 6, 7

[30] Xinyu Liu, Houwen Peng, Ningxin Zheng, Yuqing Yang, Han Hu, and Yixuan Yuan. Efficientvit: Memory efficient vision transformer with cascaded group attention. In *Proceedings of the IEEE/CVF Conference on Computer Vision and Pattern Recognition*, pages 14420–14430, 2023. 6

[31] Ze Liu, Yutong Lin, Yue Cao, Han Hu, Yixuan Wei, Zheng Zhang, Stephen Lin, and Baining Guo. Swin transformer: Hierarchical vision transformer using shifted windows. In *Proceedings of the IEEE/CVF International Conference on Computer Vision*, pages 10012–10022, 2021. 1, 3, 4, 6, 7

[32] Mindaugas Mitkus, Simon Potier, Graham R Martin, Olivier Duriez, and Almut Kelber. Raptor vision. In *Oxford Research Encyclopedia of Neuroscience*, 2018. 2

[33] Maria-Elena Nilsback and Andrew Zisserman. Automated flower classification over a large number of classes. In *2008 Sixth Indian Conference on Computer Vision, Graphics & Image processing*, pages 722–729. IEEE, 2008. 7

[34] Omkar M Parkhi, Andrea Vedaldi, Andrew Zisserman, and CV Jawahar. Cats and dogs. In *2012 IEEE Conference on Computer Vision and Pattern Recognition*, pages 3498–3505. IEEE, 2012. 7

[35] Ilija Radosavovic, Raj Prateek Kosaraju, Ross Girshick, Kaiming He, and Piotr Dollár. Designing network design spaces. In *Proceedings of the IEEE/CVF Conference on Computer Vision and Pattern Recognition*, pages 10428–10436, 2020. 6

[36] Dongyu Rao, Tianyang Xu, and Xiao-Jun Wu. Tgfuse: An infrared and visible image fusion approach based on transformer and generative adversarial network. *IEEE Transactions on Image Processing*, 2023. 1

[37] Olga Russakovsky, Jia Deng, Hao Su, Jonathan Krause, Sanjeev Satheesh, Sean Ma, Zhiheng Huang, Andrej Karpathy, Aditya Khosla, Michael Bernstein, et al. Imagenet large scale visual recognition challenge. *International Journal of Computer Vision*, 115:211–252, 2015. 2, 6

[38] Peter Shaw, Jakob Uszkoreit, and Ashish Vaswani. Self-attention with relative position representations. In *Proceedings of the 2018 Conference of the North American Chapter of the Association for Computational Linguistics: Human Language Technologies, Volume 2 (Short Papers)*, pages 464–468, 2018. 4

[39] Christian Szegedy, Vincent Vanhoucke, Sergey Ioffe, Jon Shlens, and Zbigniew Wojna. Rethinking the inception architecture for computer vision. In *Proceedings of the IEEE Conference on Computer Vision and Pattern Recognition*, pages 2818–2826, 2016. 6

[40] Mingxing Tan and Quoc Le. Efficientnet: Rethinking model scaling for convolutional neural networks. In *International Conference on Machine Learning*, pages 6105–6114. PMLR, 2019. 8

[41] Wei Tang, Fazhi He, Yu Liu, and Yansong Duan. Matr: Multimodal medical image fusion via multiscale adaptive transformer. *IEEE Transactions on Image Processing*, 31:5134–5149, 2022. 1

[42] Hugo Touvron, Matthieu Cord, Matthijs Douze, Francisco Massa, Alexandre Sablayrolles, and Hervé Jégou. Training data-efficient image transformers & distillation through attention. In *International Conference on Machine Learning*, pages 10347–10357. PMLR, 2021. 3, 6, 8

[43] Hugo Touvron, Matthieu Cord, Alexandre Sablayrolles, Gabriel Synnaeve, and Hervé Jégou. Going deeper with image transformers. In *Proceedings of the IEEE/CVF International Conference on Computer Vision*, pages 32–42, 2021. 6

[44] Hugo Touvron, Alexandre Sablayrolles, Matthijs Douze, Matthieu Cord, and Hervé Jégou. Graft: Learning fine-grained image representations with coarse labels. In *Pro*

*ceedings of the IEEE/CVF International Conference on Computer Vision*, pages 874–884, 2021. 8

[45] Zhengzhong Tu, Hossein Talebi, Han Zhang, Feng Yang, Peyman Milanfar, Alan Bovik, and Yinxiao Li. Maxvit: Multi-axis vision transformer. In *European Conference on Computer Vision*, pages 459–479. Springer, 2022. 1

[46] Grant Van Horn, Oisin Mac Aodha, Yang Song, Alexander Shepard, Hartwig Adam, Pietro Perona, and Serge Belongie. The inaturalist challenge 2017 dataset. *arXiv preprint arXiv:1707.06642*, 1(2):4, 2017. 7

[47] Ashish Vaswani, Noam Shazeer, Niki Parmar, Jakob Uszkoreit, Llion Jones, Aidan N Gomez, Łukasz Kaiser, and Illia Polosukhin. Attention is all you need. *Advances in Neural Information Processing Systems*, 30, 2017. 1, 3

[48] Cong Wang, Hongmin Xu, Xiong Zhang, Li Wang, Zhitong Zheng, and Haifeng Liu. Convolutional embedding makes hierarchical vision transformer stronger. In *European Conference on Computer Vision*, pages 739–756. Springer, 2022. 3

[49] Wenhai Wang, Enze Xie, Xiang Li, Deng-Ping Fan, Kaitao Song, Ding Liang, Tong Lu, Ping Luo, and Ling Shao. Pyramid vision transformer: A versatile backbone for dense prediction without convolutions. In *Proceedings of the IEEE/CVF International Conference on Computer Vision*, pages 568–578, 2021. 2, 3, 6, 7, 8

[50] Wenhai Wang, Enze Xie, Xiang Li, Deng-Ping Fan, Kaitao Song, Ding Liang, Tong Lu, Ping Luo, and Ling Shao. Pvt v2: Improved baselines with pyramid vision transformer. *Computational Visual Media*, 8(3):415–424, 2022. 6, 7

[51] Thomas Wolf, Lysandre Debut, Victor Sanh, Julien Chau- mond, Clement Delangue, Anthony Moi, Pierrick Cistac, Tim Rault, Rémi Louf, Morgan Funtowicz, et al. Transformers: State-of-the-art natural language processing. In *Proceedings of the 2020 Conference on Empirical Methods in Natural Language Processing: System Demonstrations*, pages 38–45, 2020. 3

[52] Haiping Wu, Bin Xiao, Noel Codella, Mengchen Liu, Xiyang Dai, Lu Yuan, and Lei Zhang. Cvt: Introducing convolutions to vision transformers. In *Proceedings of the IEEE/CVF International Conference on Computer Vision*, pages 22–31, 2021. 3, 6

[53] Zhiufan Xia, Xuran Pan, Shiji Song, Li Erran Li, and Gao Huang. Vision transformer with deformable attention. In *Proceedings of the IEEE/CVF Conference on Computer Vision and Pattern Recognition*, pages 4794–4803, 2022. 7

[54] Weijian Xu, Yifan Xu, Tyler Chang, and Zhuowen Tu. Co-scale conv-attentional image transformers. In *Proceedings of the IEEE/CVF International Conference on Computer Vision*, pages 9981–9990, 2021. 6

[55] Yifan Xu, Huapeng Wei, Minxuan Lin, Yingying Deng, Kekai Sheng, Mengdan Zhang, Fan Tang, Weiming Dong, Feiyue Huang, and Changsheng Xu. Transformers in computational visual media: A survey. *Computational Visual Media*, 8:33–62, 2022. 1

[56] Yufei Xu, Qiming Zhang, Jing Zhang, and Dacheng Tao. Vitae: Vision transformer advanced by exploring intrinsic inductive bias. *Advances in Neural Information Processing Systems*, 34:28522–28535, 2021. 8

[57] Zhixiang Xue, Xiong Tan, Xuchu Yu, Bing Liu, Anzhu Yu, and Pengqiang Zhang. Deep hierarchical vision transformer for hyperspectral and lidar data classification. *IEEE Transactions on Image Processing*, 31:3095–3110, 2022. 1

[58] Ting Yao, Yehao Li, Yingwei Pan, Yu Wang, Xiao-Ping Zhang, and Tao Mei. Dual vision transformer. *IEEE Transactions on Pattern Analysis and Machine Intelligence*, 2023. 1

[59] Kun Yuan, Shaopeng Guo, Ziwei Liu, Aojun Zhou, Feng-wei Yu, and Wei Wu. Incorporating convolution designs into visual transformers. In *Proceedings of the IEEE/CVF International Conference on Computer Vision*, pages 579–588, 2021. 3, 8

[60] Li Yuan, Yunpeng Chen, Tao Wang, Weihao Yu, Yujun Shi, Zi-Hang Jiang, Francis EH Tay, Jiashi Feng, and Shuicheng Yan. Tokens-to-token vit: Training vision transformers from scratch on imagenet. In *Proceedings of the IEEE/CVF International Conference on Computer Vision*, pages 558–567, 2021. 6

[61] Sangdoo Yun, Dongyoon Han, Seong Joon Oh, Sanghyuk Chun, Junsuk Choe, and Youngjoon Yoo. Cutmix: Regularization strategy to train strong classifiers with localizable features. In *Proceedings of the IEEE/CVF International Conference on Computer Vision*, pages 6023–6032, 2019. 6

[62] Hongyi Zhang, Moustapha Cisse, Yann N Dauphin, and David Lopez-Paz. mixup: Beyond empirical risk minimization. *arXiv preprint arXiv:1710.09412*, 2017. 6

[63] Jiangning Zhang, Xiangtai Li, Yabiao Wang, Chengjie Wang, Yibo Yang, Yong Liu, and Dacheng Tao. Eatformer: Improving vision transformer inspired by evolutionary algorithm. *arXiv preprint arXiv:2206.09325*, 2022. 1

[64] Pengchuan Zhang, Xiyang Dai, Jianwei Yang, Bin Xiao, Lu Yuan, Lei Zhang, and Jianfeng Gao. Multi-scale vision longformer: A new vision transformer for high-resolution image encoding. In *Proceedings of the IEEE/CVF International Conference on Computer Vision*, pages 2998–3008, 2021. 6

[65] Qinglong Zhang and Yu-Bin Yang. Rest: An efficient transformer for visual recognition. *Advances in Neural Information Processing Systems*, 34:15475–15485, 2021. 3, 7

[66] Zizhao Zhang, Han Zhang, Long Zhao, Ting Chen, Sercan Ö Arik, and Tomas Pfister. Nested hierarchical transformer: Towards accurate, data-efficient and interpretable visual understanding. In *Proceedings of the AAAI Conference on Artificial Intelligence*, volume 36, pages 3417–3425, 2022. 6

[67] Zhun Zhong, Liang Zheng, Guoliang Kang, Shaozi Li, and Yi Yang. Random erasing data augmentation. In *Proceedings of the AAAI Conference on Artificial Intelligence*, volume 34, pages 13001–13008, 2020. 6

[68] Xizhou Zhu, Weijie Su, Lewei Lu, Bin Li, Xiaogang Wang, and Jifeng Dai. Deformable detr: Deformable transformers for end-to-end object detection. *arXiv preprint arXiv:2010.04159*, 2020. 1